Journal of Chromatography A 1635 (2021) 461658

Contents lists available at ScienceDirect

Journal of Chromatography A

journal homepage: www.elsevier.com/locate/chroma

A methodology employing retention modeling for achieving control space in liquid chromatography method development using quality by design approach

Karthik Jayaraman [a,*], Ashok Kumar Rajendran [a], Gandhi Santosh Kumar [a], Hemant Bhutani [b,*]

[a] Analytical Research and Development, Pharmaceutical Development, Biocon Bristol Myers Squibb Research and Development Center, Syngene International Limited, Bangalore 560099, India

[b] Pharmaceutical Development, Biocon Bristol Myers Squibb Research and Development Center, Bristol Myers Squibb India Private Limited, Bangalore 560099, India

ARTICLE INFO

Article history:
Received 10 August 2020
Revised 21 October 2020
Accepted 23 October 2020
Available online 4 November 2020

Keywords:
Liquid chromatography method development
Quality by design
DryLab®
Retention modeling
In-silico optimization
Robustness evaluation

ABSTRACT

This study reports the application of retention modeling and quality by design practices for reverse-phase liquid chromatographic method development of a new chemical entity. Prior to the retention modeling, preliminary screening experiments were performed for the selection of stationary phase, organic modifiers, and method parameters. Based on the results of preliminary method conditions, t_G-T (gradient time - temperature) 2-D modeling with 4 input runs, and t_G-T-t_c (gradient time-temperature-ternary composition) 3-D modeling with 12 input runs were designed to build a model for achieving the optimized separation. Modeling of reverse phase separations was based on the measurement of both retention times and peak areas. A design space with appropriate input variables and control strategy was established prior to optimization and robustness evaluation following the quality by design framework. DryLab® was used to predict the optimized gradient profile and separation temperature. The robustness evaluation was carried out using the multiple factors at a time approach and the control space was established. The interdependence of control space and the control strategy was demonstrated by evaluating method robustness using two levels of system suitability criteria. The predictive accuracy of the retention modeling was established through experimental verification of the in-silico predictions. The quality by design based method development approach demonstrated the in-silico optimization as an integral component of reverse-phase chromatographic method development to evaluate the interplay of factors such as organic modifiers, separation temperature and gradient time, which greatly integrated and enhanced method robustness during method development.

© 2020 Elsevier B.V. All rights reserved.

1. Introduction

As per the International Council for Harmonisation of Technical Requirements for Pharmaceuticals for Human Use (ICH) guidelines Q8(R2), Quality by Design (QbD) is defined as "*systematic approach to development that begins with predefined objectives and emphasizes product and process understanding and process control, based on sound science and quality risk management*" [1]. QbD principles to the development of analytical methods are being widely adopted in the pharmaceutical industry to generate data that constitute a broad experimental space and to achieve built-in method robustness [2-5]. When the US Food and Drug Administration (FDA) first introduced QbD, its initial application included synthesis of active pharmaceutical ingredient (API), drug product formulations, and biopharmaceutical process development [6]. However, owing to the role of an analytical method in evaluating the quality of a pharmaceutical product, the QbD concepts were quickly adopted by the separation scientists [7-14]. The concept of analytical quality by design (AQbD), a systematic approach to analytical method development has effectively enabled analytical scientists to develop and validate methods that consistently provides reliable results with quality [15-17]. Vogt et al. reviewed the principles and summarized the state of QbD in the analytical method development context [18]. Both, Orlandini et al. and Vogt et al. have compared different QbD models and method development strategies that have been established to implement QbD principles and have proposed

* Corresponding authors.
E-mail addresses: karthik.j@syngeneintl.com (K. Jayaraman), hemant.bhutani@bms.com (H. Bhutani).

https://doi.org/10.1016/j.chroma.2020.461658
0021-9673/© 2020 Elsevier B.V. All rights reserved.

a QbD guide for analytical method development [18-19]. Key requirements of the QbD analytical method development process are to evaluate the robustness and ruggedness of the method, understand the critical method variables, and establish proven acceptable ranges.

QbD terms that are most pertinent to analytical method development include Design Space (DSp), Control Space (CSp) and Control Strategy (CS). As per ICH guidelines Q8 (R2) [1], DSp is defined as *"the multidimensional combination and interaction of input variables (*e.g. *material attributes) and process parameters that have been demonstrated to provide assurance of quality*". In the liquid chromatography (LC) method development context, it includes any combination of the input variables such as gradient time, % organic modifier, pH of mobile phase and separation temperature that have a bearing on the quality of the data generated by the method [13]. CSp is an area of DSp that is selected for routine operation and is dependent on the CS. As per ICH guidelines Q8(R2) [1] CS is defined as *"a planned set of controls, derived from current product and process understanding that ensures process performance and product quality"*. In the LC method development framework, CS includes the set of controls placed on the system suitability requirements (for example resolution, tailing factor, height equivalent to a theoretical plate, etc.) ensuring the method is operating consistently within the CSp.

Integration of QbD principles with the method development approach by using either empirical modeling tools (statistically based design of experiments (DoE)) such as JMP®, SAS®, Design-Expert®, and Minitab®, or mechanistic modeling tools (chromatographic retention) such as DryLab® [8-12,14,20-23], ChromSwordAuto® [24-26], ACD/AutoChrom® [27-31] have been widely reported in the last decade or so. Additionally, there are available software packages such as Fusion AE® [7,32] (QbD based software for LC method development) that serve as automated liquid chromatography method development platform with in-built formal experimental design tools. Mattrey et al. have provided a succinct review of the available chromatography simulation and modeling software packages and their core capabilities [33]. Dispas et al. have compiled an overview of QbD principles and statistical strategies (DoE-DSp approach) applied in the development of analytical methods [5]. Most researchers have discussed retention modeling and QbD based method development strategies using a model mixture of commercially available pharmaceutical compounds and reference materials [8,11,12,20,22]. To the best of our knowledge, there is a requisite for demonstrating successful implementation of retention modeling and QbD methodologies in the realm of reverse-phase method development for NCEs. In our earlier work, we proposed a stepwise method development strategy [21], where the robustness evaluation involved a univariate approach or OFAT (One Factor at a Time) approach. The main drawback of OFAT approach was that it does not account for the multiple interactions between robustness parameters thereby leading to overestimation of the true CSp. In the current work, we attempt to evaluate the method robustness by creating a DSp in a multivariate approach or MFAT (Multiple Factors at a Time) approach to arrive at a CSp. MFAT approach results in analytical method with robust ranges of operation and hence minimizes the risk of failure when the analytical method is transferred from the development environment into a GMP testing quality control laboratory for supporting production and life cycle management of the product. The method development, optimization, robustness verification and identification of a routine CSp were achieved through the following steps:

- Established a preliminary analytical method through the evaluation of selected method parameters
- Established DSp and an optimized analytical method using two-dimensional (t_G-T) and three- dimensional (t_G-T-t_c) modeling
- Performed (predicted) method robustness verification following MFAT approach with two levels of CS (system suitability criteria) using DryLab®
- Determined CSp based on the robustness results

The sample for this study consisted of an API from our internal discovery program, its process-related impurity (A), and two diastereomers of the API (B, C). The development of the method described in this paper was particularly challenging as the impurities present in the sample were structurally very similar to the API itself. It is important to note that the case study in this paper involving separation of API from 3 other impurities is representative of an analytical method associated with new drug application (NDA) submission and at this juncture the process is fully optimized, locked and the batches are clean with very minimal impurities.

2. Experimental

2.1. Chemicals

API and its isomers were synthesized by the Chemical Development and API Supply group in Biocon Bristol Myers Squibb Research and Development Center (BBRC), Bangalore, India. HPLC grade methanol (MeOH) and acetonitrile (MeCN) were procured from S.D. Fine Chemicals (SD Fine, Mumbai, India) and Rankem (Rankem, New Delhi, India) respectively. Trifluroacetic acid (TFA) and ammonium acetate (NH_4OAc) were obtained from Biosolve Chimie (Dieuze, France). Water was obtained using an in house Milli-Q system (Millipore Sigma, Massachusetts, USA). A sample marker mixture was prepared from the individual components such that the API was present at a concentration of 0.5 mg/mL and the other compounds (A, B, and C) were present at approximately 0.2 to 0.8 area percent (AP) relative to API. MeCN:Water (80:20 v/v) was used as the sample diluent and sample injection volume was 5µL.

2.2. HPLC columns

The HPLC columns (listed in Table S1) used in this study were purchased from the respective vendors.

2.3. Eluents

Two pairs of eluents were used for column screening analysis (Section 3.1 and 3.2) and they were as below: 1) pH ~ 2.0, A = 0.05% v/v TFA in Water: MeOH (90:10 v/v); B = 0.05% v/v TFA in MeCN:MeOH (90:10 v/v) and 2) pH ~ 6.5, A = 0.01 M NH_4OAc in Water:MeOH (90:10 v/v); B = 0.01 M NH_4OAc in Water:MeCN:MeOH (10:80:10v/v/v). For t_G-T and tG-T-tc modeling input experiments, eluent A was 0.05% v/v TFA in 100% water, and eluent B was 0.05% v/v TFA with varying ratios of MeCN & MeOH. Throughout this study t_c refers to the % of MeOH in eluent B.

2.4. Instrumentation and software

Chromatographic evaluation and measurements were made using an A1200 HPLC system equipped with a diode array detector (Agilent Technologies, Santa Clara, CA, USA). The dwell volume was measured to be 1.36 mL. Waters (Milford, MA, USA) Empower Software (Feature Release 2) was used to acquire, store, and process the chromatographic data. Retention times and peak areas of individual peaks from experimental runs were used as input data for DryLab® v.4.0 chromatography optimization software (Molnar Institut, Berlin Germany). Robustness of the method was predicted

Table 1
Chromatographic system suitability requirements for the resolution (control strategy).

Level	Criteria
1 (Required)	Resolution between A and API $\geq$ 1.5; Resolution between API and *B* $\geq$ 1.5; Resolution between B and *C* $\geq$ 1.5
2 (Desired)	Resolution between A and API $\geq$ 2.0; Resolution between API and *B* $\geq$ 2.0; Resolution between B and *C* $\geq$ 2.0

Table 2
Preliminary and final optimized LC method conditions.

Parameter	Preliminary Method Conditions	Final Optimized Method Conditions
Column	Ascentis Express C18 (150 × 4.6) mm, 2.7 µ	Ascentis Express C18 (150 × 4.6) mm, 2.7 µ
Eluent pH	2.0	2.0
Organic Modifier	Eluent A: 0.05% v/v TFA in Water Eluent B: 0.05% v/v TFA in 100% MeOH or 100% MeCN or MeOH:MeCN (1:1 v/v)	Eluent A: 0.05% v/v TFA in Water Eluent B: 0.05% v/v TFA in MeOH: MeCN (40:60 v/v)
Column Temperature (T)	35 °C	35 °C
Wavelength	254 nm	254 nm
Flow Rate	1.0 ml per minute	1.0 ml per minute
Gradient Time (t_G)	40 min	45 min
Initial Organic	10% B	10% B
Final Organic	100% B	100% B

using DryLab® v.4.0 using a 4-factor- 2 level full factorial design and was experimentally verified.

2.5. Design space (DSp), control strategy (CS) and control space (CSp)

The DSp was established using the combination of variables namely t_G, T, and t_c that were the most influencing parameters (critical parameters) in determining the quality of the method being developed in this work. It is important to note that the other critical parameter, eluent pH, was not chosen to be an influencing parameter based on preliminary analytical method selection experiments discussed in Section 3.2. In this work, CS was the chromatographic system suitability requirement for the resolutions as listed in Table 1. CSp is a portion of DSp driven by the CS controls and the method is validated to ensure that it is robust and operates in the CSp without any failure.

3. Results and discussion

3.1. Analytical method development strategy

AQbD starts with clearly defining the analytical target profile (ATP) or method goals, and one may choose the analytical technique(s) that can meet the method goals. In this study, ATP was defined as an analytical method with adequate baseline separation of all the impurities (see Table 1 for resolution requirements) and establishing a design space, in which the method is robust. Reversed phase liquid chromatography was chosen as the technique, which is well suited to meet the ATP pre-requisites. A preliminary LC method to resolve closely eluting structurally related impurities in an active pharmaceutical ingredient was obtained using a simplified method development strategy that consisted of column screening, eluent pH screening, organic modifier selection, temperature, and gradient time optimization. The columns and eluent screening were performed concurrently at eluent pH values of ~2.0 and 6.5 (for details see Section 2.3), column temperature of 30 °C, flow rate of 1.0 mL/minute, and wavelength of 254 nm. The parameter F in Table S1 indicates the similarity between columns, and it is derived using the USP-PQRI approach which is based on the hydrophobic subtraction model of reverse-phase column selectivity [34]. Using this approach values of $F>3$ can be used to select columns with different selectivity and in this study, values of F for the columns selected for screening ranged between 4.7 (Waters XBridge C18) and 23.0 (Waters XSelect HSS PFP). The organic modifier selection (MeOH vs MeCN) was initially simplified by adding 10% v/v MeOH to eluents A and B in the screening experiments. Hence the LC method development was focused on achieving selectivity through the identification of a suitable stationary phase, appropriate eluent pH, selecting a practical organic modifier and finally performing software-assisted fine optimization (for T, t_G,% t_c) of the selected method.

3.2. Preliminary analytical method selection

Column screening at two different eluent pH values revealed that pH did not have any significant influence on the separation of peaks. The selection of the column chemistry and pH was based on the number of peaks detected, and the resolution between peaks (A & API and API & B or C) as listed in Table S2. It is important to note that only C18 stationary phases (with F values of 4.7 and 8.5) offered the separation of all peaks and all other columns with F values above 8.5 did not yield separation of all peaks. The acceptable and comparable separation was achieved with Ascentis Express C18 at both pH 2.0 and 6.5; and hence taking into practical considerations, this stationary phase with TFA containing eluent was selected for further method development. Figure S1 and S2 show the overlay of the chromatograms from column screening at pH 2 and 6.5 respectively. Table 2 contains the preliminary method condition that was used as an input condition for DryLab® optimization in the next step. Since MeOH was present as an organic modifier in addition to MeCN during the initial screening experiments, it was important to optimize the ternary composition of the eluent using DryLab®.

3.3. DryLab® optimization of the preliminary method

Modeling of reverse phase separations by DryLab® is based on the measurement of both retention times and peak areas. In this work, DryLab® was used to predict the optimized gradient profile, separation temperature, and ternary composition of the mobile phase. Experimental design for simultaneous optimization of gradient time(t_G) and temperature (T) required four experiments as follows: *Run 1*: 20-minutes gradient at 25 °C, *Run 2*: 60-minutes gradient at 25 °C, *Run 3*: 20-minutes gradient at 50 °C and *Run 4*: 60-minutes gradient at 50 °C. Following the recommended input con-

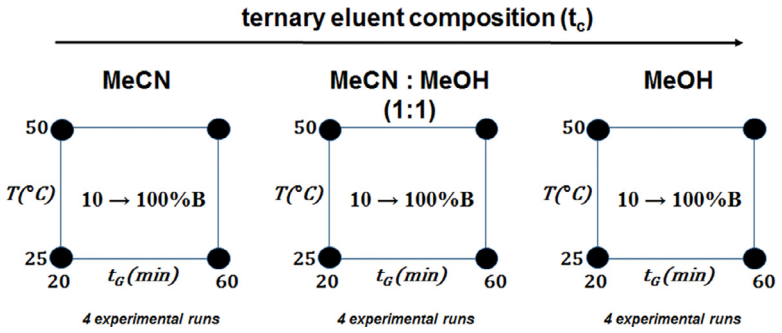

Fig. 1. Experimental design for a 3-dimensional LC method optimization. 3 t_G-T modeling with 4 experimental runs in each and 1 t_G-T-t_c modeling with 4 × 3 experimental runs. t_G is gradient time, T is column temperature and t_c is ternary composition.

ditions for DryLab® predictions, the two gradient times differ by a factor of 3 and the ΔT of the two column temperatures is 25 °C. A wide gradient range of 10 – 100% B was chosen for all four runs thereby enabling exploration of deeper and broader DSp. The two-dimensional t_G-T modeling with the same set of four input experiments was performed using pure MeCN, pure MeOH and 1:1v/v (MeCN: MeOH) as the organic modifier in eluent B. The twelve input experiments together constituted the 3-dimensional modeling (t_G-T-t_c) with gradient time, column temperature and ternary composition as model variables (Fig. 1).

3.3.1. t_G-T retention modeling

As discussed in Section 3.3, t_G-T modeling was performed with three different organic modifiers (eluent B) and chromatograms from all the 12 experiments are shown in Fig. 2 wherein (a) with MeCN as the organic modifier, experiments 1 & 3 and 2 & 4 provided the same separation which indicated that column temperature had no impact on the separation. However, the resolution between API and B was significantly improved between experiments 1 & 2 and 3 & 4 which suggested that gradient steepness (run time of 20 vs 60 min) greatly influenced the resolution. In (b) with MeOH as the organic modifier, the selectivity was altered leading to elution of impurity A after the API. At higher column temperature, the resolution between API and A was reduced compared to lower column temperature as seen from experiments 1 & 3. Similarly, the resolution between A and B was reduced at higher column temperature as seen from experiments 2 & 4. The elution order change between peaks API & A and longer retention times for all components when MeOH is used could be correlated to the difference in the retention mechanism i.e., adsorption like for water:MeCN and partition like for water:MeOH mixtures. In (c) with MeOH and MeCN (1:1 v/v) as the organic modifier, experiments 1 & 2 and 3 & 4 indicated that gradient steepness (run time of 20 vs 60 min) had no major influence on the resolution of API and impurity A. However, comparison of experiments 1 & 3 and 2 & 4 indicated that resolution between A and API was significantly improved at lower column temperature. Fig. 2(d) provides the predicted chromatograms for the DryLab® suggested optimized condition for each organic modifier selection. Peaks that are colored red in each predicted chromatogram indicate the critical peak pairs. The predicted resolution between critical pairs were 1.66 (B and C), 2.30 (API and A) and 2.54 (B and C) using 100% MeCN, 100% MeOH and 1:1 v/v (MeCN:MeOH) as organic modifiers respectively. Fig. 3 shows the two-dimensional resolution maps of gradient time, t_G, [min] against the column temperature T [°C] for each of the 3 experimental sets. Calculated peak resolutions of 0.00–1.60, 0.00–2.34 and 0.00–2.17 in increments of 0.02, 0.43 and 0.47 for Fig. 3(a), (b), and (c), respectively, are shown as color-coded regions and give a visual representation of the robustness of the separation. The black arrow in each of the resolution map in Fig. 3 denotes the DryLab® suggested optimized condition for that organic modifier selection.

At this juncture, there were three optimized method conditions, i.e., one condition for each ternary eluent composition. Therefore, selecting a single ternary eluent composition and finalizing the method with the DryLab® suggested optimized conditions would have restricted the DSp and compromised the method robustness. With the intent of a) establishing a broader DSp, b) identifying the right ratio of MeCN to MeOH (ternary composition) that triggers the selectivity (between A and API) change and c) understanding the role of ternary composition in the overall optimization of the separation, a 3D modeling (t_G-T-t_c) study was explored. As shown in Fig. 1, the 12 input experiments that were already performed as part of t_G-T modeling were leveraged to obtain the predicted data for t_G-T-t_c modeling.

3.3.2. t_G-T-t_c retention modeling

In this 3D modeling, gradient time (t_G), temperature (T) and eluent ternary composition (t_c) were selected as model variables to create a cube resolution map that predicted the critical resolution of the peaks to be separated. 3D resolution spaces as shown in Fig. 4 represent the simultaneous influence of three parameters on selectivity and critical resolution. Fig. 4(a) through (f) shows the t_G–T–ternary resolution space at a selected t_c. As shown in Fig. 4, the % of MeOH in eluent B plays a critical role in establishing an acceptable DSp. The DSp was found to be broad and considered acceptable at t_c values of 100% (Fig. 4a), 40% (Fig. 4d) and 20% (Fig. 4e). The DSp was found to be narrow and slightly acceptable at t_c values of 60% (Fig. 4c) and 0% (Fig. 4f). The DSp was almost none and unacceptable at t_c value of 80% (Fig. 4b). To further substantiate the selection of t_c value, DryLab® was used to predict the separation of the peaks for conditions with t_c values ranging from 0% to 100% MeOH in intervals of 10% as shown in Fig. 5(a) through (k). These predicted chromatograms provide a detailed picture of how the selectivity and resolution varied with varying % of t_c. As seen in Fig. 5, the resolution between API & B and B & C continue to increase from 0% MeOH to 50% MeOH and peaks B & C remain as critical pair (colored in red). As t_c value changed from 50% to 60% MeOH, the resolution between A and API diminished and at t_c values of 70% and 80% MeOH, A & API completely co-eluted. At t_c value of 90% MeOH, the order of elution between A & API changed and they emerged as a critical pair. At t_c value of 100% MeOH, the separation between API & A improved and A & B emerged as critical pair. This understanding of peak movement (elution order) and critical peak pairs was possible due to the detailed (t_G-T-t_c) 3D modeling and this would not have been understood only by the (t_G-T) 2D modeling approach.

3.3.3. Final DryLab® optimized method condition and establishing DSp

Table 3 lists the DryLab® predicted peak retention time (t_R) and resolution (R_s) between the critical peak pairs at various t_c values. Based on the CS, *i.e.*, system suitability criteria (level 1) defined in Table 1, t_c values that led to predictions 8, 9 &10 were neglected. Prediction 11 with 100% MeOH in eluent B was not preferred since higher MeOH content leads to higher UV background and higher back-pressure. Prediction 1 with 0% MeOH was not chosen since it is evident that MeOH plays a significant role in selectivity and achieving higher resolution based on discussions in Section 3.3.1. Predictions 6 and 7 were not preferred since the critical peak pair changes from B & C (prediction 6,%t_c = 60) to A & API (prediction 7,%t_c = 70), which will impact the method robustness. In comparing predictions 2, 3, 4 & 5, prediction 5 has the highest resolution for the critical pair and meets the system suitability resolution criterion for the other two peak pairs too. This outcome was also evident from the three-dimensional resolution

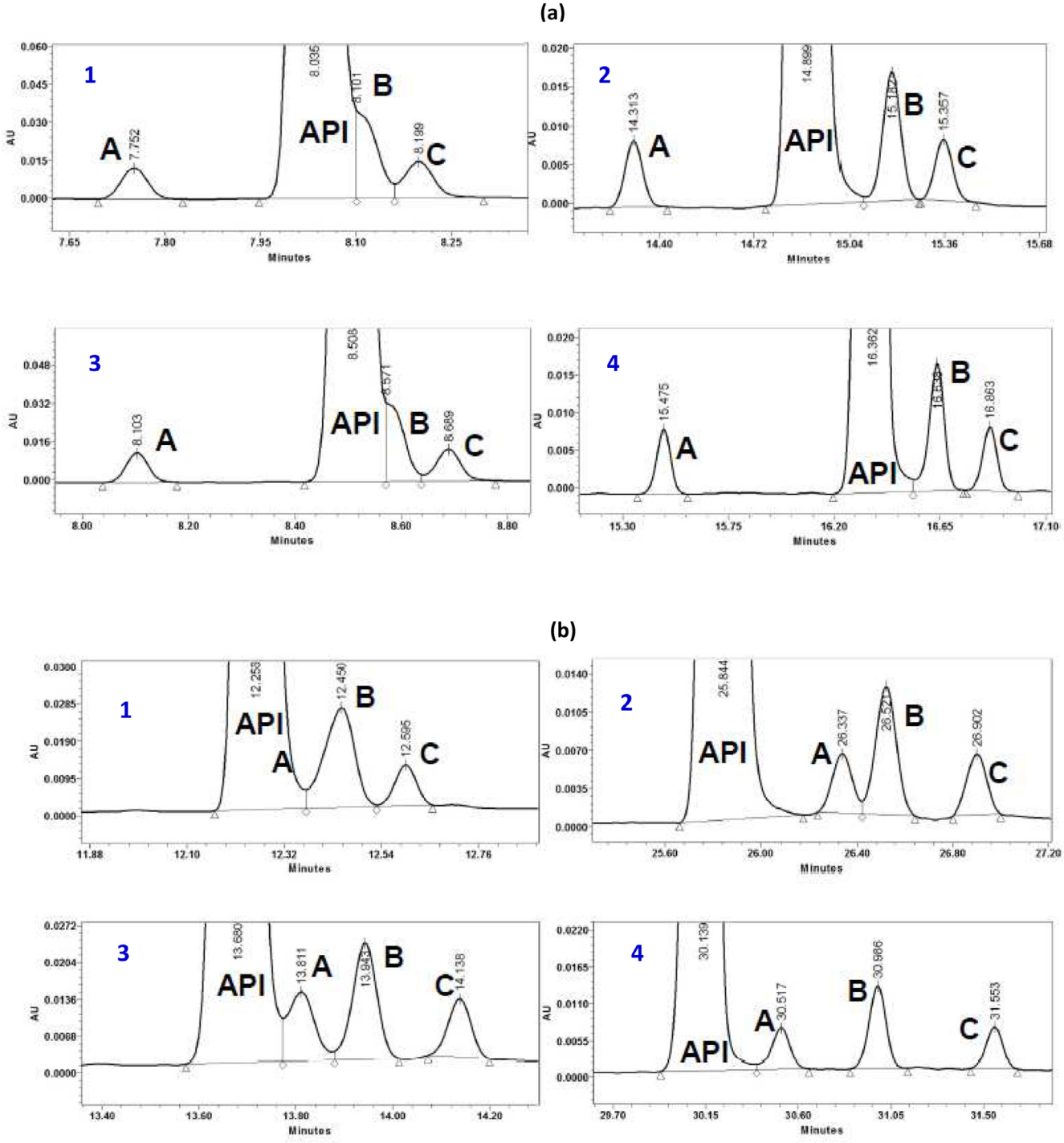

Fig. 2. Experimental chromatograms showing influence of gradient time and column temperature on separation of API and related peaks. Chromatographic parameters as listed in Table 2 (preliminary method conditions). a) Eluent B is 100% MeCN, b) Eluent B is 100% MeOH and c) Eluent B is 1:1 v/v (MeOH: MeCN); 1: 20 min & 50 °C, 2: 60 min & 50 °C, 3: 20 min & 25 °C, 4: 60 min & 25 °C. d) DryLab® predicted chromatograms (inset: zoomed chromatograms) for the optimized conditions based on t_G-T modeling. t_G is gradient time and T is column temperature.

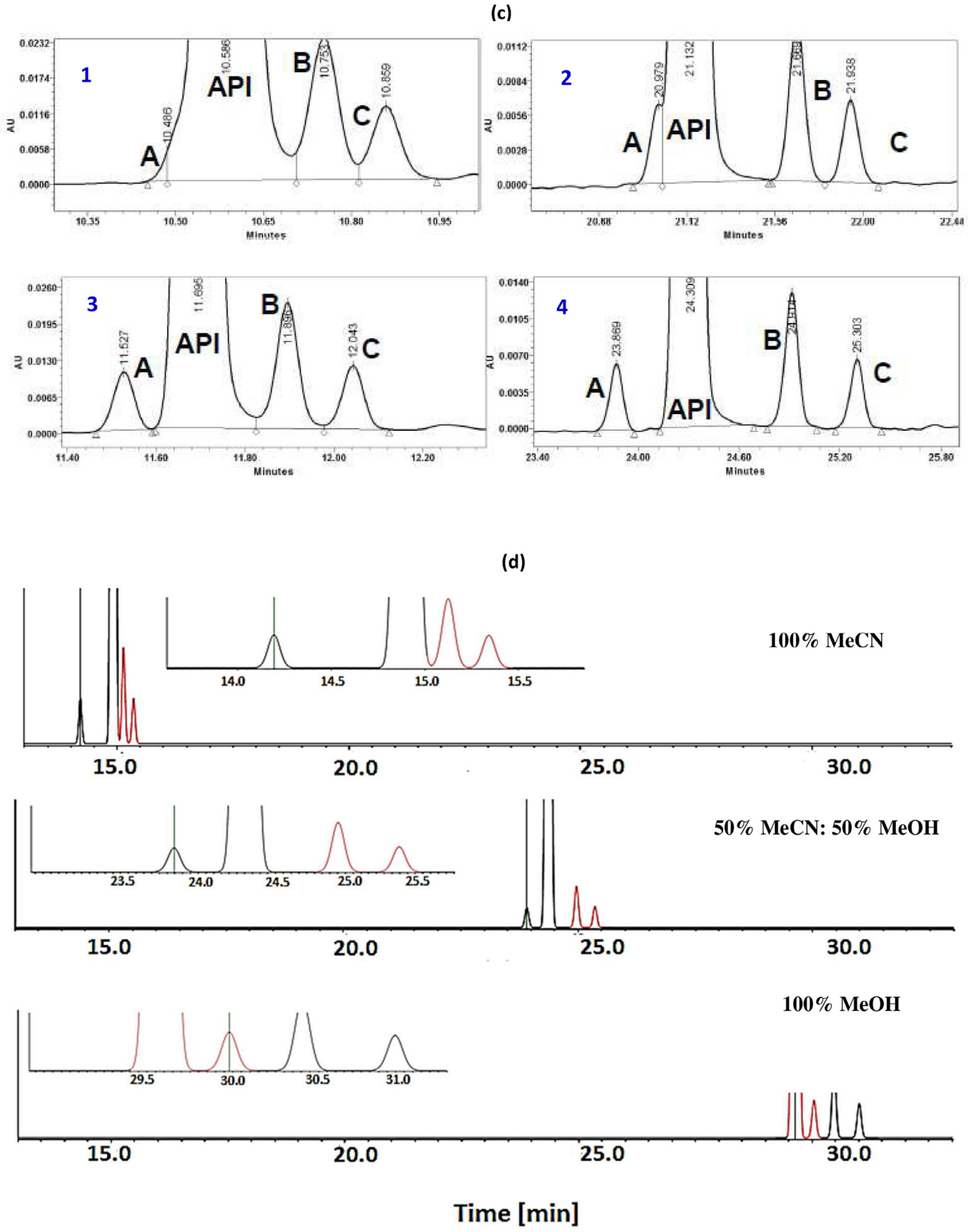

Fig. 2. Continued

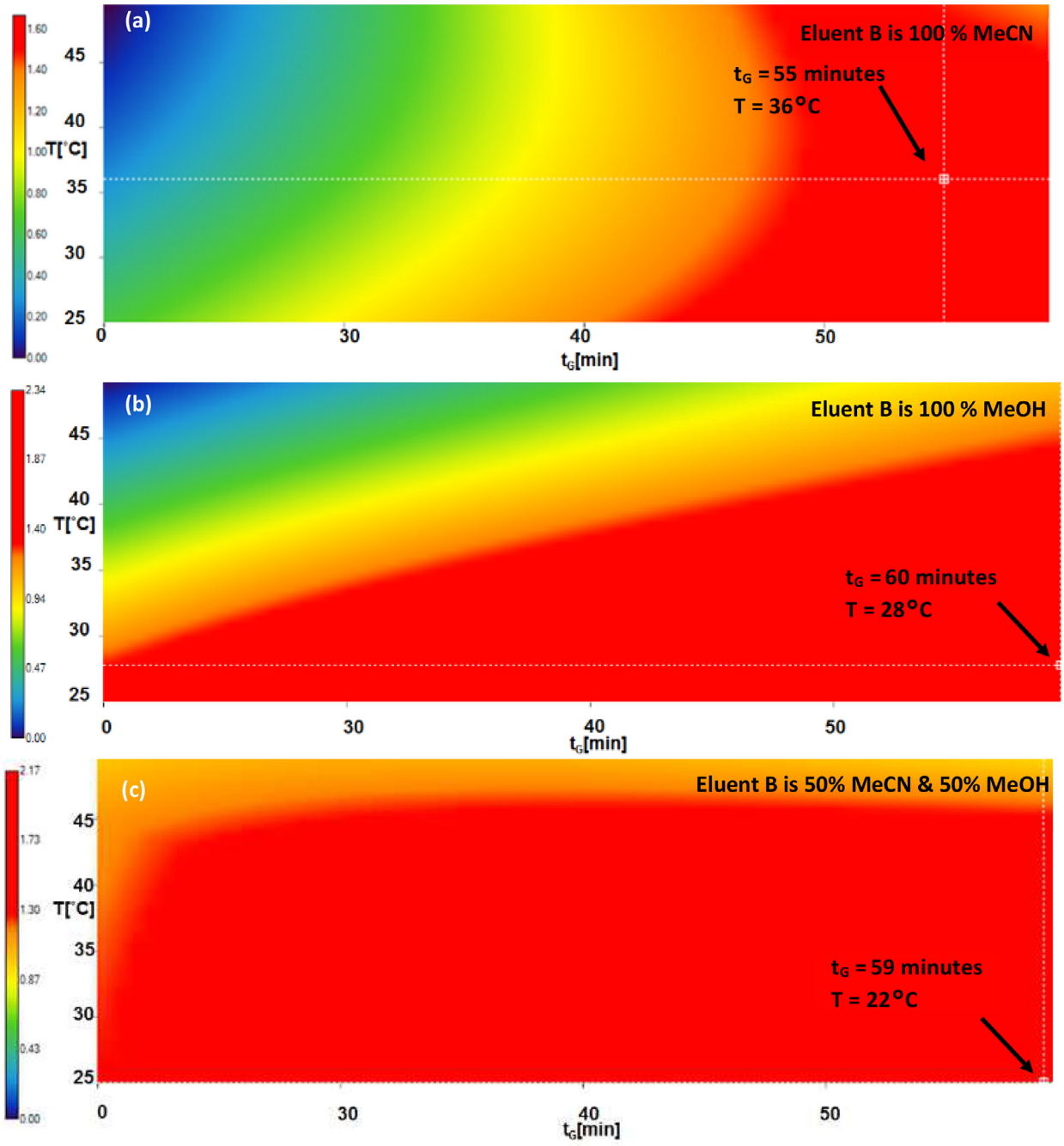

Fig. 3. Two-dimensional resolution maps of gradient time, t_G, [min] against the column temperature T [°C] for each of the nine experimental sets. See Table 2 (preliminary method conditions) for other method conditions employed. t_G, T and organic modifier (eluent B) were as listed in the resolution map. t_G is gradient time and T is column temperature.

space map in Fig. 4d. The resolution table (shown in Fig. 6a) provides an alternative display of the resolution as a function of gradient time and temperature matrix. The black-lined boundary indicates the DSp within which a reasonable separation ($R_S \geq 1.5$) can be obtained with the critical pair always being B & C (designated as 3, 4). For example, for a t_G of 45 min and a temperature of 35 °C, a resolution of 1.87 is predicted for the critical pair B & C (see highlighted entry in Fig. 6a). If an optimized condition has to be selected only by achieving the highest resolution for the critical pair, a gradient time of 60 min and a temperature of 23 °C (R_S = 2.19) would have been the final method condition. However, for practical reasons with respect to the effective control of the column temperature and to achieve a broader DSp, a gradient time of 45 min and a temperature of 35 °C (condition is shown by the dotted line in Fig. 6b) were selected as the most robust conditions from this analysis and these values were employed as the final optimized condition (Table 2). Fig. 4(d) suitably illustrates the established DSp. To summarize, the finalized t_G-T-t_c values were 45 min-35 °C-40%, respectively, and these set of values not only define a set point, but represent a broader DSp, in which stable QbD-relevant routine is feasible with increased flexibility.

3.3.4. *Experimental verification of DryLab® optimized method*

To verify the DryLab® prediction, an experiment was carried out using the final optimized conditions as summarized in Table 2. The predictive ability of the DryLab® was evaluated by compar-

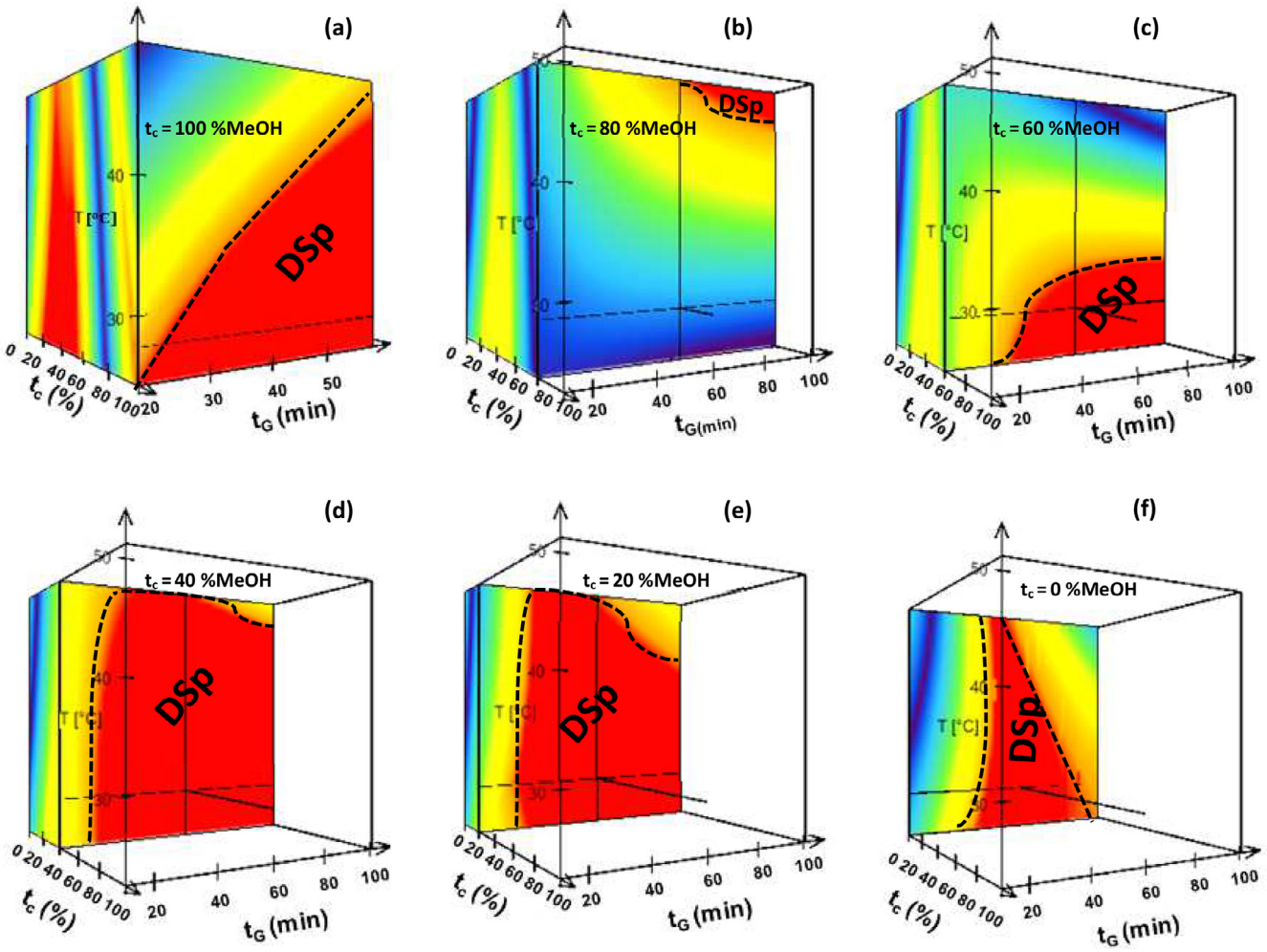

Fig. 4. Three-dimensional resolution space maps of t_G[min] - T[°C] - t_c(%) modeling and design space (DSp) at specific t_c. (a), (b), (c), (d), (e) and (f) corresponds to t_c of 100%, 80%, 60%, 40%, 20% and 0% methanol in eluent B. Space (colored in red) within the black dotted lines corresponds to DSp. See Table 2 (preliminary method conditions) for other method conditions employed. t_G is gradient time, T is column temperature and t_c is ternary composition. (For interpretation of the references to colour in this figure legend, the reader is referred to the web version of this article.)

Table 3
DryLab® predicted retention time of peaks and resolution for critical peak pairs at various t_c (% methanol in eluent B).

Prediction #	t_c (%MeOH in eluent B)	R_s (A & API)	R_s (API & B) or R_s (A & B)	R_s (B & C)	t_R of peak			
					A	API	B	C
1	0	6.25	1.98	**1.61**	15.2	16.0	16.4	16.5
2	10	5.47	2.35	**1.76**	16.9	17.7	18.0	18.3
3	20	4.73	2.68	**1.89**	18.6	19.3	19.6	19.8
4	30	4.01	2.99	**2.01**	20.3	20.8	21.3	21.6
5	40	3.27	3.27	**2.13**	21.8	22.3	22.8	23.2
6	50	2.50	3.53	**2.27**	23.3	23.6	24.2	24.5
7	60	**1.66**	3.79	2.42	24.6	24.8	25.5	26.0
8	70	**0.75**	4.06	2.60	26.0	26.0	26.7	27.1
9	80	**0.23**	4.10	2.79	27.1	27.1	27.9	28.4
10	90	**1.27**	3.34	3.01	**28.4**	**28.2**	29.0	29.5
11	100	**2.35**	2.55	3.23	**29.7**	**29.3**	30.0	30.5

R_s highlighted in bold are critical peak pairs at the given t_c; t_R highlighted in bold indicates change in elution order.

ing the predicted and experimentally obtained retention times and resolutions (Table 4). The compared retention times were in good agreement, with the average of the errors being 1.8% and similar levels of predictive accuracy for DryLab®, in terms of retention time have been reported by Guichard et al. [20], Kormany et al. [14].and Schmidt et al. [22]. The compared resolution values were also in good agreement, with the average of the errors being 5.1%. Slightly higher errors for resolution values as compared to retention time is not atypical and has been previously reported by Jayaraman et al. [21] and Fekete et al. [35]. More importantly, the predicted and experimental resolution for the critical pair (B & C) were in excellent agreement with an absolute difference of only

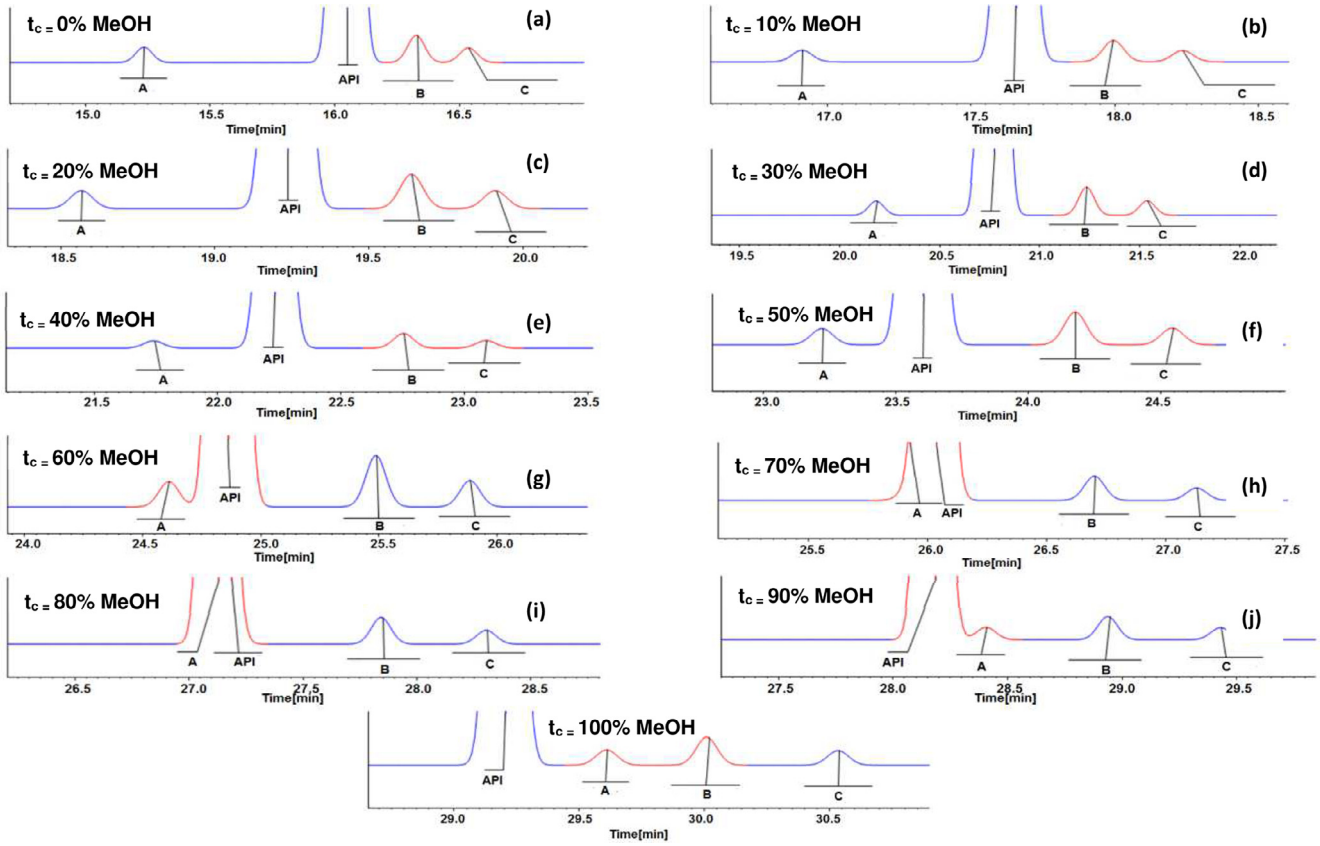

Fig. 5. DryLab® predicted chromatograms showing influence of tc (% methanol in eluent B) on selectivity and resolution of critical pairs. t_G of 60 min & T of ~30 °C was kept constant for all predictions. Other chromatographic parameters as listed in Table 2 (preliminary method conditions). t_G is gradient time, T is column temperature and t_c is ternary composition. (For interpretation of the references to colour in this figure legend, the reader is referred to the web version of this article.)

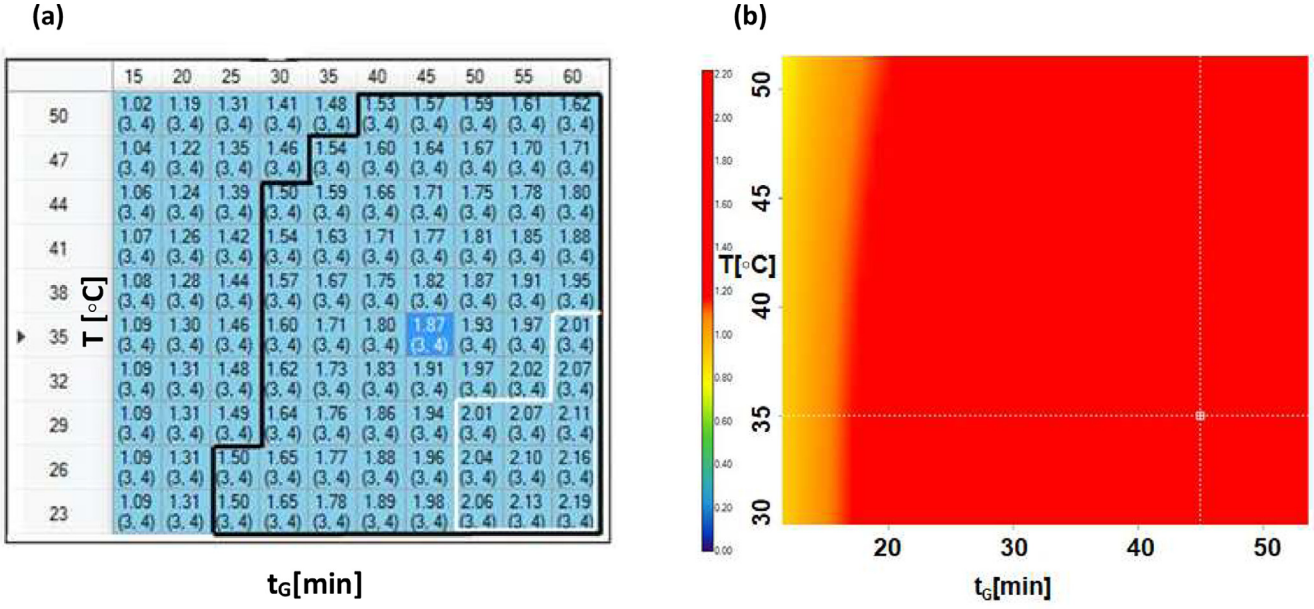

Fig. 6. (a) DryLab® 2-D resolution table and (b) DryLab® resolution map obtained for the separation to predict the final optimized separation conditions at $\%t_c$=40. Peaks B & C are designated as 3 & 4 in the resolution table. t_G is gradient time and T is column temperature. (For interpretation of the references to colour in this figure legend, the reader is referred to the web version of this article.)

0.04. It should be noted that the error in resolution prediction is a resultant of the error in retention time prediction combined with the uncertainty in peak width prediction [21]·[35]. The chromatograms from the DryLab® prediction and the verification experiment are shown in Fig. 7 for visual comparison.

3.4. Robustness verification and defining CSp

While evaluating the built-in method robustness as part of method development, DryLab® was used to predict the robustness of the optimized method listed in Table 2. The method robustness was verified with two different levels of CS (system suitability cri-

Table 4
DryLab® predicted and experimental value for the resolution and retention time.

Peak Identity	Retention time (minutes)				Resolution (R_s)			
	Predicted	Experimental	Difference[a]	% Error[b]	Predicted	Experimental	Difference[a]	% Error[b]
A	17.56	17.26	0.30	1.71	NA	NA	NA	NA
API	17.92	17.59	0.33	1.84	2.92	2.76	0.16	5.48
B	18.3	17.97	0.33	1.80	3.04	3.28	0.24	7.89
C	18.55	18.20	0.35	1.89	2.03	2.07	0.04	1.97
		Average	0.33	1.8		Average	0.15	5.11

[a] Difference = experimental – predicted.
[b] % Error = [(experimental – predicted)/predicted] x 100.

Table 5
Chromatographic parameters and range for robustness verification.

Parameter	Low	Center (actual method condition)	High
t_G, Gradient Time (min)	40	45	50
Initial Organic (%)	5	10	15
T, Temperature (°C)	30	35	40
t_c, Ternary Composition (% MeOH in eluent B)	30	40	50

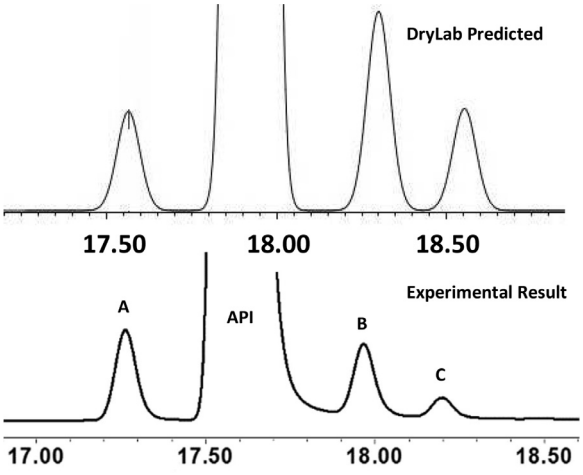

Fig. 7. DryLab® predicted and experimentally obtained chromatograms (using DryLab® optimized separation conditions). See Table 2 for final optimized method conditions employed.

teria) as listed in Table 1. The method robustness was verified by changing four selected chromatographic parameters (t_G, T, t_c and% initial organic) within a range of approximately ± 10% to ± 50% of the method condition (see Table 5) using MFAT approach. For the MFAT approach, 20 experiments (16 different conditions and actual method condition repeated 4 times) were generated using 4 factor 2-level factorial design as shown in Table 6. The outcome of the 20 experiments was predicted by DryLab® and verified experimentally too. DryLab® was used to predict all three resolutions for all conditions and these values were compared with the experimental results as shown in Table 6. Using the robustness module in DryLab®, the CSp was also predicted in 3-D space as shown in Fig. 8. The red-colored region (CSp) represents the space where all the resolution criteria were met, while the empty region (outside CSp) represents the space where the method failed to meet all the resolution criteria. It is to be noted that the CSp is bound to the CS (resolution criteria in this work) and when the CS is altered or modified, the CSp will change accordingly. For example, when the system suitability criteria were changed from required (level 1) to desired (level 2) as listed in Table 1, the CSp changed as seen in Figure 8 (a) and (b). This was also evident from the 2D resolution table in Fig. 6(a), where the black-lined boundary indicated the CSp for level 1 criteria and the white-line boundary indicated the CSp for level 2 criteria. For level 1 criteria, the entire DSp was available as CSp, while for level 2 criteria, only a small portion of DSp was available as CSp.

3.4.1. Interdependence between CSp and CS

The three experimental resolution values were all above 1.5, and all experiments satisfied level 1 (required) criteria as defined in Table 1. While evaluating the robustness using level 2 (desired) criteria, 8 out of the 16 varied conditions failed to meet the system suitability criteria. Out of these 8 failed experiments, 4 experiments have $R_s < 2.0$ for B & C, 2 experiments have $R_s < 2.0$ for A & API and remaining 2 experiments have $R_s < 2.0$ for both A & API and B & C (see Table 6). The difference in resolution between the deliberate change and the actual method condition, which reflect the robustness of the method, were all within an acceptable range with the average difference (absolute) being 0.7, 0.3 and 0.2 for A & API, API & B, and B & C respectively over the 20 measurements shown in Table 6. The method was robust in the entire DSp with level 1 system suitability criteria (i.e., DSp same as CSp), while, the method was not robust in the entire DSp with level 2 system suitability criteria (i.e., only a portion of DSp is CSp) This difference in the robustness space was also evident from Fig. 8(a) and (b) as discussed in Section 3.3.3. Figure S3 shows the frequency distribution of the critical pair R_s (experimental value) for the MFAT based robustness evaluation conditions. The success rate of all 16 experiments (varied conditions) meeting the system suitability criteria was 100% for level 1 (Figure S3a) and 50% for level 2 (Figure S3b). This approach of evaluating the method robustness using 2 sets of system suitability criteria further corroborates the fact that the success of a method within the established DSp was dependent on the CS associated with the method.

3.4.2. Predictive accuracy of DryLab®

Out of the 16 varied conditions in the robustness evaluation, the critical pair was A & API for 4 experiments and B & C for 12 experiments. The critical pairs remained the same in DryLab® prediction and experimental results. The DryLab® predicted resolution values for the peak pairs were all in good agreement with the experimental values, with the average error being 9.1%, 6.7% and 4.8% for A & API, API & B and B & C, respectively, over the 20 measurements shown in Table 6. The % error of predicted accuracy was positive (predicted lower than experimental) for A & API and negative (experimental lower than predicted) for API & B and combination of positive and negative for B & C. Any adjustment over the plate number during the DryLab® predictions would im-

Table 6
Resolution values obtained for robustness verification.

Experiment #	A:t_G, Gradient Time min	B:Initial Organic %	C:T, Temperature °C	D:t_c,% methanol) %	Predicted			Experimental			% Error (Predictive Accuracy)			Difference (Method Robustness)		
					Rs (A and API)	Rs (API and B)	Rs (B and C)	R_s (A and API)	R_s (API and B)	R_s (B and C)	R_s (A and API)	R_s (API and B)	R_s (B and C)	R_s (A and API)	R_s (API and B)	R_s (B and C)
1	40	5	30	30	3.9	2.7	2.0	3.8	2.8	2.0	2.3	−5.3	1.5	1.1	−0.5	−0.1
2	50	15	30	30	4.1	3.0	2.1	4.1	3.3	2.1	2.2	−8.6	0.0	1.3	0.0	0.1
3[a]	45	10	35	40	2.9	3.0	2.0	2.8	3.3	2.1	5.5	−7.9	−2.0	0.0	0.0	0.0
4[f]	40	5	40	50	1.8	3.0	1.9	**1.5**	3.1	**1.9**	17.7	−3.0	2.6	−1.3	−0.2	−0.2
5[f]	40	15	40	30	3.4	2.6	1.9	3.0	2.7	**1.7**	11.0	−4.7	12.9	0.2	−0.6	−0.4
6	50	5	30	30	4.1	2.9	2.1	4.1	3.2	2.2	0.0	−8.9	−4.3	1.3	−0.1	0.1
7	40	5	30	50	2.3	3.2	2.1	2.0	3.4	2.2	15.1	−5.0	−6.2	−0.8	0.1	0.2
8	50	5	30	50	2.4	3.5	2.2	2.1	3.8	2.4	12.0	−9.9	−7.6	−0.6	0.5	0.3
9[f]	50	15	40	50	1.8	3.4	2.0	**1.6**	3.6	2.0	15.2	−5.9	−0.5	−1.2	0.3	0.0
10[f]	40	5	40	30	3.3	2.5	1.9	3.0	2.6	**1.7**	9.7	−5.7	12.6	0.2	−0.7	−0.4
11	50	15	30	50	2.5	3.6	2.3	2.2	4.0	2.5	12.1	−11.3	−8.3	−0.6	0.7	0.4
12[f]	40	15	40	50	1.8	3.1	2.0	**1.5**	3.2	**1.9**	19.0	−2.6	2.6	−1.3	−0.1	−0.2
13[a]	45	10	35	40	2.9	3.0	2.0	2.8	3.3	2.1	5.5	−7.9	−2.0	0.0	0.0	0.0
14[f]	50	5	40	30	3.3	2.8	1.9	3.2	3.0	**1.8**	4.2	−6.5	5.7	0.4	−0.3	−0.3
15	40	15	30	30	4.0	2.8	2.1	3.9	2.9	2.0	4.0	−5.4	1.0	1.1	−0.4	0.0
16[a]	45	10	35	40	2.9	3.0	2.0	2.8	3.3	2.1	5.5	−7.9	−2.0	0.0	0.0	0.0
17[f]	50	15	40	30	3.4	2.9	2.0	3.2	3.0	**1.8**	7.4	−4.9	10.3	0.4	−0.3	−0.3
18	40	15	30	50	2.4	3.3	2.2	2.0	3.6	2.3	14.7	−6.6	−6.9	−0.7	0.3	0.3
19[a]	45	10	35	40	2.9	3.0	2.0	2.8	3.3	2.1	5.5	−7.9	−2.0	0.0	0.0	0.0
20[f]	50	5	40	50	1.8	3.3	2.0	**1.6**	3.5	2.1	14.3	−8.0	−5.0	−1.2	0.3	0.0

% Error = [(experimental−predicted)/predicted] × 100, used to assess predictive accuracy of DryLab®.
Difference = (R_{exp} −R_{amc}), used to assess method robustness, where R_{exp} is the experimental resolution obtained at any varied condition and R_{amc} is the resolution obtained under the actual method condition[a].
[f] Experiments which failed the level 2 system suitability criteria. Failed resolution values are in bold.

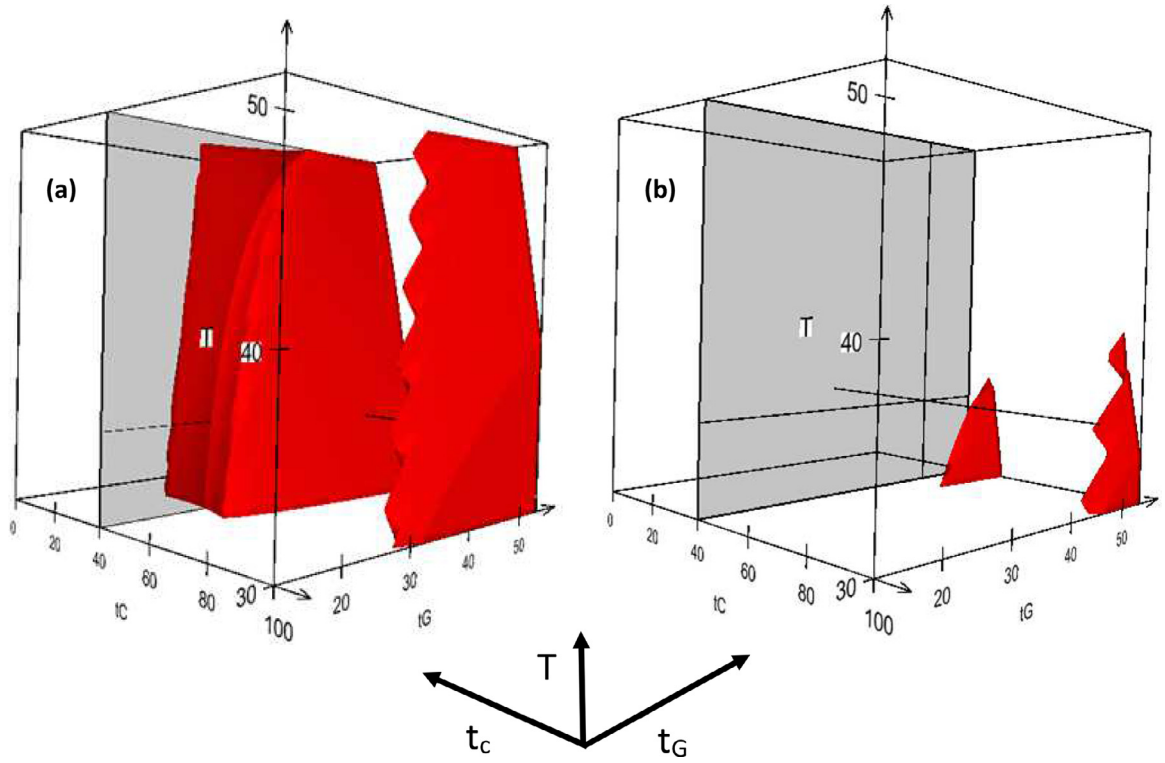

Fig. 8. (a) DryLab® cube illustrating the control space (CSp) or robust zones where (a) $R_s \geq 1.5$ (level 1, Table 1) and (b) $R_s \geq 2.0$ (level 2, Table 1).

Table 7
Analytical figures of merit for validation of optimized method.

Test	Acceptance Criteria	Result	
Specificity	Resolve critical impurities	Resolution of impurities achieved	Pass
Linearity[a]	R squared must exceed 0.995	R squared = 1.000	Pass
Precision (sample repeatability)	RSD ≤ 2.5%	RSD = 1.2% (n = 3)	Pass
Precision (injection repeatability)	RSD ≤ 1.27%	RSD = 0.03% (n = 6)	Pass
Sensitivity	RSD ≤ 15% at QL	RSD = 4%	
		QL ≤ 0.05%	Pass

RSD: Relative standard deviation ; QL: Quantitation Limit
. [a]Range from 0.05% to 150% of the working concentration.

prove the predictive accuracy of the model. The correlation between predicted and experimental resolution values is illustrated in Figure S4a and R^2 values of greater than 0.8 indicate a strong positive correlation. The correlation between predicted and experimental retention times is illustrated in Figure S4b and R^2 values of greater than 0.995 further validate the accuracy of the model. These results demonstrate that retention modeling-based simulation in DryLab® can be used with reasonable accuracy to predict the outcome of such robustness studies.

3.5. Validation of the final optimized method

In compliance with the USP <1225>[36], ICH Q2(R1) [37], the method was validated for the following parameters: method specificity, linearity, injection repeatability, sample repeatability, and sensitivity of impurities. The method was validated with the level 1 CS or system suitability criteria (Table 1) since the CSp was robust for this level. Table 7 provides the analytical figures of merit for the validation of the method. The acceptance criteria provided in Table 7 were established in the validation protocol prior to starting the validation. The results were all within the acceptance criteria. Based on the QbD based method development, the robustness of the method was already in-built within the method and the validation becomes a simple exercise that demonstrated the method is suitable for its intended purpose.

4. Conclusions

This manuscript describes the application of a retention modeling and QbD based analytical method development approach to separate the components of a structurally complex new chemical entity (NCE) containing process impurity and diastereomers of the API. The first step was to perform a preliminary screening using simplified method development strategy and leveraging the knowledge space from previous methodologies. This step was then followed by retention modeling optimization through the use of DryLab® which included 2D and 3D modeling to understand the influence of organic modifier, separation temperature and gradient time on the chromatographic separation. The optimization was performed within the QbD framework, clearly establishing the DSp, CS and achieving the CSp. The robustness of the optimized method conditions was evaluated using the MFAT approach through full factorial design at two levels of CS or system suitability criteria. The demonstration of the interdependence of CSp and CS is a significant effect, which reinforces the conclusions by previous researchers [8-12,14,21,22,24,27,38,39]. The results from the robustness experiments demonstrated that DryLab® predictions can

be significantly relied upon to determine the method robustness space and in-silico optimization is truly a green analysis initiative as it saves time, energy (instrument usage) and reduces waste (solvent consumption). The in-built robustness of the method made the validation experiments merely an iterative exercise and the validation of the final method was performed and included for the completeness of method development.

Declaration of Competing Interest

The authors declare that they have no known competing financial interests or personal relationships that could have appeared to influence the work reported in this paper.

CRediT authorship contribution statement

Karthik Jayaraman: Conceptualization, Methodology, Formal analysis, Data curation, Writing - original draft, Writing - review & editing, Visualization, Supervision. **Ashok Kumar Rajendran:** Methodology, Validation, Investigation, Data curation, Visualization. **Gandhi Santosh Kumar:** Validation, Investigation, Resources. **Hemant Bhutani:** Conceptualization, Writing - review & editing, Visualization, Supervision, Project administration, Funding acquisition.

Acknowledgements

Authors thank Dr. Lakshmikant Bajpai for valuable suggestions and review of the manuscript. Authors would also like to thank Dr. Moolchand Kurmi for important discussions on quality by design aspects. Authors acknowledge Jay Brumfield and Joel Young of Bristol Myers Squibb for their support and Syngene International Limited for providing all infrastructure support to perform this work.

Supplementary materials

Supplementary material associated with this article can be found, in the online version, at doi:10.1016/j.chroma.2020.461658.

References

[1] ICH Q8, (R2) – Guidance for Industry, Pharmaceutical DevelopmentInternational Conference on Harmonization, 2009.
[2] H. Bhutani, M. Kurmi, S. Beg, S. Singh, B. Singh, Quality by Design (QbD) in analytical sciences: an overview, Pharma Times 46 (2014) 71–75.
[3] D.K. Lloyd, J. Bergum, Chapter 3 - Application of quality by design (QbD) to the development and validation of analytical methods, in: C.M. Riley, T.W. Rosanske, S.R.R. Riley (Eds.), Specification of Drug Substances and Products, Elsevier: Oxford, 2014, pp. 29–72.
[4] P. Ramalingam, B. Jahnavi, Chapter 5 - QbD Considerations for Analytical Development, in: S. Beg, M.S. Hasnain (Eds.), Pharmaceutical Quality by Design, Academic Press, 2019, pp. 77–108.
[5] A. Dispas, H.T. Avohou, P. Lebrun, P. Hubert, C. Hubert, Quality by Design' approach for the analysis of impurities in pharmaceutical drug products and drug substances, Trends Analyt Chem 101 (2018) 24–33.
[6] https://www.fda.gov/regulatory-information/search-fda-guidance-documents/q8r2-pharmaceutical-development (accessed June 2020).
[7] R. Mallik, S. Raman, X. Liang, A.W. Grobin, D. Choudhury, Development and validation of a rapid ultra-high performance liquid chromatography method for the assay of benzalkonium chloride using a quality-by-design approach, J Chromatogr A 1413 (2015) 22–32.
[8] I. Molnár, H.J. Rieger, K.E. Monks, Aspects of the "Design Space" in high pressure liquid chromatography method development, J Chromatogr A 1217 (19) (2010) 3193–3200.
[9] K. Monks, I. Molnár, H.J. Rieger, B. Bogáti, E. Szabó, Quality by Design: multidimensional exploration of the design space in high performance liquid chromatography method development for better robustness before validation, J Chromatogr A 1232 (2012) 218–230.
[10] K.E. Monks, H.J. Rieger, I. Molnár, Expanding the term "Design Space" in high performance liquid chromatography (I), J Pharm Biomed Anal 56 (5) (2011) 874–879.
[11] N. Rácz, I. Molnár, A. Zöldhegyi, H.-J. Rieger, R. Kormány, Simultaneous optimization of mobile phase composition and pH using retention modeling and experimental design, J Pharm Biomed Anal 160 (2018) 336–343.
[12] A. Zöldhegyi, H.J. Rieger, I. Molnár, L. Fekhretdinova, Automated UHPLC separation of 10 pharmaceutical compounds using software-modeling, J Pharm Biomed Anal 156 (2018) 379–388.
[13] E. Rozet, P. Lebrun, P. Hubert, B. Debrus, B. Boulanger, Design Spaces for analytical methods, Trends Analyt Chem 42 (2013) 157–167.
[14] R. Kormány, I. Molnár, H.J. Rieger, Exploring better column selectivity choices in ultra-high performance liquid chromatography using Quality by Design principles, J Pharm Biomed Anal 80 (2013) 79–88.
[15] R. Deidda, S. Orlandini, P. Hubert, C. Hubert, Risk-based approach for method development in pharmaceutical quality control context: a critical review, J Pharm Biomed Anal 161 (2018) 110–121.
[16] R. Peraman, K. Bhadraya, Y. Padmanabha Reddy, Analytical quality by design: a tool for regulatory flexibility and robust analytics, Int J Anal Chem 2015 (2015) 868727.
[17] T. Tome, N. Žigart, Z. Časar, A. Obreza, Development and optimization of liquid chromatography analytical methods by using AQbD principles: overview and recent advances, Org Process Res Dev 23 (9) (2019) 1784–1802.
[18] F.G. Vogt, A.S. Kord, Development of quality-by-design analytical methods, J Pharm Sci 100 (3) (2011) 797–812.
[19] S. Orlandini, S. Pinzauti, S. Furlanetto, Application of quality by design to the development of analytical separation methods, Anal Bioanal Chem 405 (2) (2013) 443–450.
[20] N. Guichard, S. Fekete, D. Guillarme, P. Bonnabry, S. Fleury-Souverain, Computer-assisted UHPLC–MS method development and optimization for the determination of 24 antineoplastic drugs used in hospital pharmacy, J Pharm Biomed Anal 164 (2019) 395–401.
[21] K. Jayaraman, A.J. Alexander, Y. Hu, F.P. Tomasella, A stepwise strategy employing automated screening and DryLab modeling for the development of robust methods for challenging high performance liquid chromatography separations: a case study, Anal. Chim. Acta 696 (1) (2011) 116–124.
[22] A.H. Schmidt, M. Stanic, I. Molnár, In silico robustness testing of a compendial HPLC purity method by using of a multidimensional design space build by chromatography modeling—Case study pramipexole, J Pharm Biomed Anal 91 (2014) 97–107.
[23] A.H. Schmidt, I. Molnár, Using an innovative Quality-by-Design approach for development of a stability indicating UHPLC method for ebastine in the API and pharmaceutical formulations, J Pharm Biomed Anal 78-79 (2013) 65–74.
[24] K.P. Xiao, Y. Xiong, F.Z. Liu, A.M. Rustum, Efficient method development strategy for challenging separation of pharmaceutical molecules using advanced chromatographic technologies, J Chromatogr A 1163 (1) (2007) 145–156.
[25] J. Zheng, A.M. Rustum, Rapid separation of desloratadine and related compounds in solid pharmaceutical formulation using gradient ion-pair chromatography, J Pharm Biomed Anal 51 (1) (2010) 146–152.
[26] E.F. Hewitt, P. Lukulay, S. Galushko, Implementation of a rapid and automated high performance liquid chromatography method development strategy for pharmaceutical drug candidates, J Chromatogr A 1107 (1) (2006) 79–87.
[27] L. Wang, J. Zheng, X. Gong, R. Hartman, V. Antonucci, Efficient HPLC method development using structure-based database search, physico-chemical prediction and chromatographic simulation, J Pharm Biomed Anal 104 (2015) 49–54.
[28] J.D. Stafford, T.D. Maloney, D.P. Myers, J.M. Cintron, B.C. Castle, A systematic approach to development of liquid chromatographic impurity methods for pharmaceutical analysis, J Pharm Biomed Anal 56 (2) (2011) 280–292.
[29] Haidar Ahmad, I. A., W. Chen, H.M. Halsey, A. Klapars, J. Limanto, G.F. Pirrone, T. Nowak, R. Bennett, R. Hartman, A.A. Makarov, I. Mangion, E.L. Regalado, Multi-column ultra-high performance liquid chromatography screening with chaotropic agents and computer-assisted separation modeling enables process development of new drug substances, Analyst 144 (9) (2019) 2872–2880.
[30] R. Bennett, I.A. Haidar Ahmad, J. DaSilva, M. Figus, K. Hullen, F.-.R. Tsay, A.A. Makarov, B.F. Mann, E.L. Regalado, Mapping the separation landscape of pharmaceuticals: rapid and efficient scale-up of preparative purifications enabled by computer-assisted chromatographic method development, Org Process Res Dev 23 (12) (2019) 2678–2684.
[31] Haidar Ahmad, I. A., V. Shchurik, T. Nowak, B.F. Mann, E.L. Regalado, Introducing multifactorial peak crossover in analytical and preparative chromatography via computer-assisted modeling, Anal. Chem. 92 (19) (2020) 13443–13451.
[32] S. Karmarkar, R. Garber, Y. Genchanok, S. George, X. Yang, R. Hammond, Quality by design (QbD) based development of a stability indicating HPLC method for drug and impurities, J Chromatogr Sci 49 (6) (2011) 439–446.
[33] F.T. Mattrey, A.A. Makarov, E.L. Regalado, F. Bernardoni, M. Figus, M.B. Hicks, J. Zheng, L. Wang, W. Schafer, V. Antonucci, S.E. Hamilton, K. Zawatzky, C.J. Welch, Current challenges and future prospects in chromatographic method development for pharmaceutical research, Trends Analyt Chem 95 (2017) 36–46.
[34] PQRI Approach for Selecting Columns of Equivalent Selectivity https://www.usp.org/resources/pqri-approach-column-equiv-tool (accessed July 2020).
[35] S. Fekete, J. Fekete, I. Molnár, K. Ganzler, Rapid high performance liquid chromatography method development with high prediction accuracy, using 5cm long narrow bore columns packed with sub-2μm particles and Design Space computer modeling, J Chromatogr A 1216 (45) (2009) 7816–7823.
[36] http://www.pharmacopeia.cn/v29240/usp29nf24s0 c1225.html (accessed July 2020).

[37] https://www.fda.gov/regulatory-information/search-fda-guidance-documents/q2-r1-validation-analytical-procedures-text-and-methodology (accessed July 2020).
[38] B. Debrus, P. Lebrun, J.M. Kindenge, F. Lecomte, A. Ceccato, G. Caliaro, J.M.T. Mbay, B. Boulanger, R.D. Marini, E. Rozet, P. Hubert, Innovative high-performance liquid chromatography method development for the screening of 19 antimalarial drugs based on a generic approach, using design of experiments, independent component analysis and design space, J Chromatogr A 1218 (31) (2011) 5205–5215.
[39] B. Debrus, D. Guillarme, S. Rudaz, Improved quality-by-design compliant methodology for method development in reversed-phase liquid chromatography, J Pharm Biomed Anal 84 (2013) 215–223.